nature climate change

LETTERS

PUBLISHED ONLINE: 11 JANUARY 2016 | DOI: 10.1038/NCLIMATE2914

Response of marine bacterioplankton pH homeostasis gene expression to elevated CO_2

Carina Bunse[1], Daniel Lundin[1], Christofer M. G. Karlsson[1], Neelam Akram[1†], Maria Vila-Costa[2†], Joakim Palovaara[1†], Lovisa Svensson[1], Karin Holmfeldt[1], José M. González[3], Eva Calvo[4], Carles Pelejero[4,5], Cèlia Marrasé[4], Mark Dopson[1], Josep M. Gasol[4] and Jarone Pinhassi[1*]

Human-induced ocean acidification impacts marine life. Marine bacteria are major drivers of biogeochemical nutrient cycles and energy fluxes[1]; hence, understanding their performance under projected climate change scenarios is crucial for assessing ecosystem functioning. Whereas genetic and physiological responses of phytoplankton to ocean acidification are being disentangled[2–4], corresponding functional responses of bacterioplankton to pH reduction from elevated CO_2 are essentially unknown. Here we show, from metatranscriptome analyses of a phytoplankton bloom mesocosm experiment, that marine bacteria responded to lowered pH by enhancing the expression of genes encoding proton pumps, such as respiration complexes, proteorhodopsin and membrane transporters. Moreover, taxonomic transcript analysis showed that distinct bacterial groups expressed different pH homeostasis genes in response to elevated CO_2. These responses were substantial for numerous pH homeostasis genes under low-chlorophyll conditions (chlorophyll $a < 2.5\,\mu g\,l^{-1}$); however, the changes in gene expression under high-chlorophyll conditions (chlorophyll $a > 20\,\mu g\,l^{-1}$) were low. Given that proton expulsion through pH homeostasis mechanisms is energetically costly, these findings suggest that bacterioplankton adaptation to ocean acidification could have long-term effects on the economy of ocean ecosystems.

Anthropogenic emissions of CO_2 have caused a significant decrease in oceanic surface pH, from 8.2 in pre-industrial times to a present value of 8.1 (ref. 5). Further reductions of 0.3 to 0.4 pH units are projected to occur by the end of this century[6], potentially causing pronounced changes in the oceanic carbon cycle[4]. Recent research on the ecophysiology of individual model algal species and on the structure and function of phytoplankton assemblages demonstrates both positive and negative effects of reduced pH on ocean primary producers[7]. Similarly, the magnitude of responses in bacterioplankton activity and community composition to reductions in seawater pH varies considerably between experimental studies carried out in different waters and seasons[8–13]. Given that bacterioplankton account for 12–59% of the surface ocean respiration[14], they play a critical role in regulating global biogeochemical cycles of many vital elements[1]. Yet, mechanistic understanding of physiological responses of bacterioplankton to changes in seawater pH is poor[15]. This imposes profound limitations in predicting how ocean acidification will affect bacterioplankton involvement in biogeochemical cycling.

To investigate bacterioplankton (including Bacteria, Cyanobacteria and Archaea) responses to projected ocean acidification, we carried out a mesocosm experiment with water from the Mediterranean Sea. As nutrients are central to determining ocean productivity, we chose to maintain mesocosms under two distinct trophic conditions: sea water with naturally low-nutrient concentrations versus sea water with nutrient-induced phytoplankton blooms. Under these conditions, a pH reduction of approximately 0.2 units compared with controls was obtained through controlled CO_2 bubbling (Fig. 1). Chlorophyll *a* concentrations (a proxy for phytoplankton biomass) in the natural seawater mesocosms slowly increased during the experiment from $0.6 \pm 0.1\,\mu g\,l^{-1}$ to $2.3 \pm 0.2\,\mu g\,l^{-1}$ (hereafter, low-chlorophyll (Low-Chl) mesocosms). In the nutrient-enriched mesocosms, chlorophyll *a* increased owing to phytoplankton growth and peaked at $28.4 \pm 4.1\,\mu g\,l^{-1}$ on Day 7, and then decreased until Day 9 (hereafter, high-chlorophyll (High-Chl) mesocosms). Following peaks on Day 3–5, bacterial heterotrophic production and abundance in both Low- and High-Chl mesocosms had minima on Day 7, with values increasing again until Day 9 independently of elevated CO_2 (two-tailed *t*-test, $p > 0.05$; ref. 16). A previous study on 16S ribosomal RNA gene distributions established that elevated CO_2 did not affect the relative abundance of any bacterial population in the Low-Chl mesocosms, and only two bacterial populations responded to acidification in the High-Chl mesocosms[17]. This provided a unique opportunity to directly determine whether or how natural bacterioplankton adjust their gene expression patterns to elevated CO_2 under contrasting trophic states.

Sequencing of community messenger RNA obtained at the end of the mesocosm experiment (Day 9) yielded between 4 and 11 million annotated sequence reads per sample (Supplementary Table 1), resulting in identification of 15,798 genes. Grouping of gene transcripts into functional metabolic categories showed an overall dominance of genes related to protein metabolism, membrane transport, and RNA metabolism (Supplementary Fig. 1). Taxonomic assignment of transcripts showed that Gammaproteobacteria dominated in both Low- and High-Chl mesocosms (30–53% of

[1]Centre for Ecology and Evolution in Microbial Model Systems, EEMiS, Linnaeus University, Barlastgatan 11, 391 82 Kalmar, Sweden. [2]Group of Limnology, Department of Continental Ecology, Centre d'Estudis Avançats de Blanes-CSIC, Accés Cala Sant Francesc 14, 17300 Blanes, Catalonia, Spain. [3]Department of Microbiology, University of La Laguna, 38200 La Laguna, Spain. [4]Departament de Biologia Marina i Oceanografia, Institut de Ciències del Mar—CSIC, Pg. Marítim de la Barceloneta 37-49, 08003 Barcelona, Catalonia, Spain. [5]Institució Catalana de Recerca i Estudis Avançats (ICREA), 08010 Barcelona, Catalonia, Spain. †Present addresses: Department of Biosciences, COMSATS Institute of Information Technology, 44000 Islamabad, Pakistan (N.A.); Department of Environmental Chemistry, IDAEA-CSIC, Jordi Girona 18-24, 08034 Barcelona, Catalunya, Spain (M.V.-C.); Department of Agrotechnology and Food Sciences, Wageningen University, 6703HA Wageningen, The Netherlands (J.P.). *e-mail: jarone.pinhassi@lnu.se

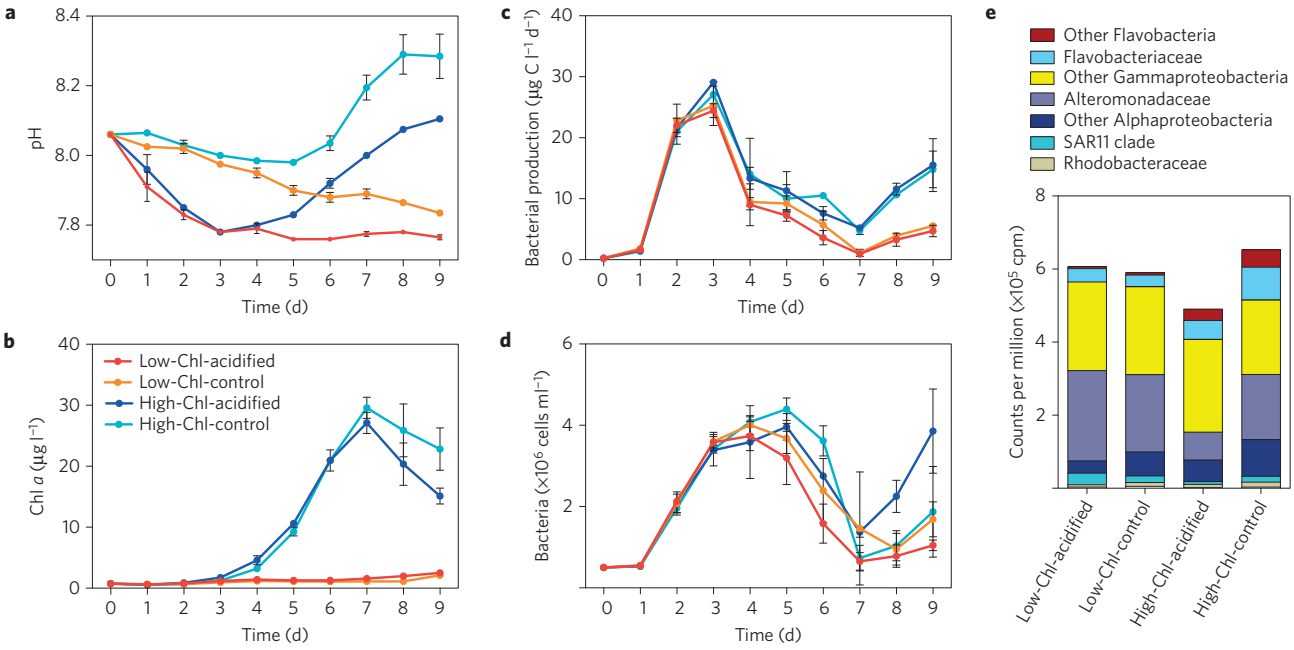

Figure 1 | Changes in pH and microbiological parameters during the mesocosm experiments. a, pH levels. **b**, Chlorophyll *a* concentrations. **c**, Bacterial heterotrophic production estimated by leucine incorporation. **d**, Bacterial abundance. **e**, Distribution of average relative RNA transcript abundances (normalized to counts per million; CPM) among the four most abundant microbial taxa (averages for duplicate mesocosms). Data in **a**–**d** represent averages of duplicate samples ± s.d. Data for panels **a**–**c** from ref. 16.

annotated reads; Fig. 1e). The abundances of Alphaproteobacteria transcripts were similar in all mesocosms (around 9%), but Bacteroidetes transcripts were ∼4% compared with 11% in the Low-Chl compared with the High-Chl mesocosms, respectively. Ribosomal protein transcripts represented around half of the 50 most abundant genes (Supplementary Fig. 2). This was in line with the measured bacterial production, indicating that bacteria in both Low- and High-Chl mesocosms were metabolically active.

Statistical analyses identified 303 genes (1.9% of total genes) in the Low-Chl mesocosms with significant differences in relative transcript abundance (that is, number of transcript reads per total annotated reads per sample) when comparing acidified with control mesocosms. Among these, 113 genes had higher abundance whereas the remaining 190 genes had lower abundance in the acidified compared with control mesocosms (EdgeR, $p < 0.01$; Fig. 2, Supplementary Fig. 3 and Supplementary Table 2). In contrast, only 54 genes (0.3% of total genes) in the High-Chl mesocosms exhibited significant differences in relative transcript abundance, 27 of which were higher in the High-Chl-acidified mesocosms (Fig. 2 and Supplementary Fig. 3 and Supplementary Table 3). This suggests that elevated CO_2 had more pronounced effects on bacterioplankton gene expression in the Low-Chl mesocosms.

In the Low-Chl mesocosms, genes with higher relative transcript abundance in the acidified compared with control mesocosms belonged to different cellular categories (Fig. 2). Remarkably, several RNA transcripts assigned to the category 'respiration' reached their highest relative abundance in the Low-Chl-acidified mesocosms (Fig. 2), and were among the most highly expressed transcripts (Supplementary Fig. 2). In particular, all five electron transport complexes were represented by at least one gene each that had significantly more RNA transcripts in the Low-Chl-acidified mesocosms (Fig. 3 and Supplementary Table 2). This included the highly expressed transmembrane subunit C for H^+ translocation in ATP synthase (complex V). In *Enterococcus hirae*, a similar F_1F_0-ATPase extrudes H^+ from the cytoplasm to regulate internal pH, rather than to generate ATP (ref. 18). Moreover, the B and E subunits of the Na^+-translocating NADH-quinone reductase were highly expressed. In several marine bacteria, this reductase is functionally analogous to the canonical proton pumping respiratory complex I, essential for energy transduction and growth of bacteria in low-salinity environments[19]. In several neutralophilic and acidophilic bacteria, an important strategy to maintain desired intracellular pH in response to acid stress (resulting from passive proton influx) is to translocate protons across the membrane through respiratory proton pumps[20,21]. This suggests that the observed pH-induced transcriptional responses in respiration-related genes in the acidified Low-Chl mesocosms would not be primarily for the bacteria to increase their respiration rates (that is, for energetic purposes), but rather as a strategy to cope with pH stress.

The most highly expressed gene with significantly different transcript levels in the acidified Low-Chl mesocosms encoded the light-driven proton pump proteorhodopsin. The proton motive force resulting from proteorhodopsin generates energy for cellular processes improving growth and survival[22,23]. It has been speculated that proteorhodopsin could be involved in modulating the response of marine bacteria to ocean acidification[24]. Our findings emphasize that proteorhodopsin-mediated proton export may contribute to pH homeostasis in marine bacteria under elevated CO_2.

In our experiment, the relative expression of some constituents of the cyanobacterial photosynthetic proton pumping and electron transfer machinery was significantly higher in the acidified compared with control Low-Chl mesocosms; including components of the photosystem I and II, light harvesting complex I, and cytochrome b_6–f complex subunit b_6. In contrast, cyanobacterial photosynthesis transcripts not part of proton pumping activities (for example, pigment synthesis genes) were relatively less expressed in Low-Chl-acidified, whereas the expression of RuBisCO genes remained unaffected by acidification. Membrane transporters accounted for 13.7% of differentially expressed genes. Nine transporter genes with assigned roles in pH homeostasis showed higher expression in the acidified Low-Chl mesocosms, including genes encoding the glutamate/aspartate transport system permease protein GltK and a proton/glutamate

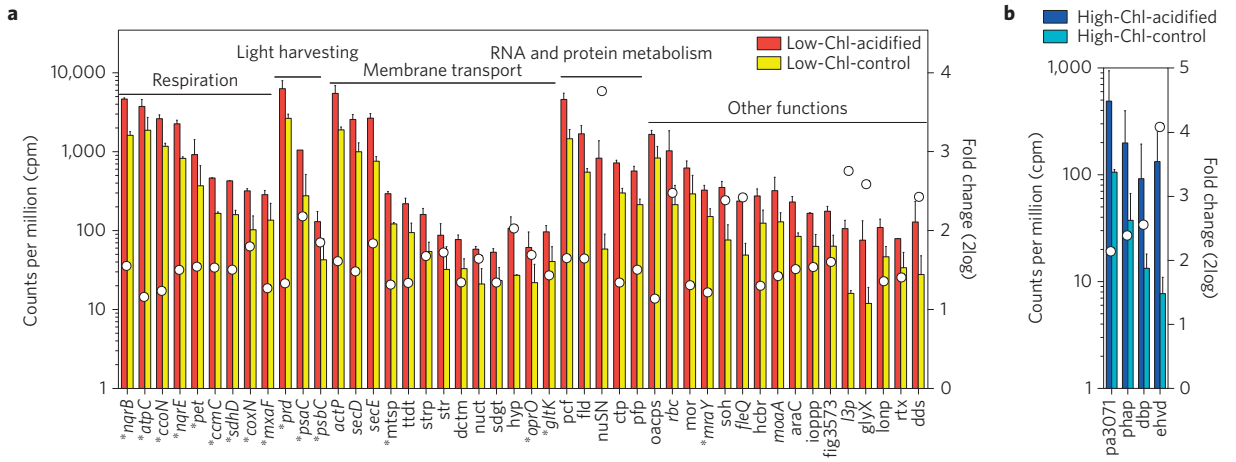

Figure 2 | Bacterioplankton gene expression response under elevated CO_2. a, Low-Chl mesocosms. **b**, High-Chl mesocosms. The figure shows average relative RNA transcript abundance (normalized to counts per million; CPM) ± standard deviations for genes with significantly higher relative abundance in acidified mesocosms compared with controls. The most abundant genes (that is, with >500 counts) are shown; all significantly differentially expressed genes are listed in Supplementary Tables 2 and 3. Transcripts with assigned roles in pH homeostasis or pH stress are denoted by asterisks. Open circles denote the logarithm base 2 of the fold change. Statistical analysis was done using EdgeR (p value < 0.01); considering only transcripts for which CPM values from each replicate in acidified mesocosms was 1.5 times the average of non-acidified controls. Full gene names for the gene abbreviations are shown in Methods.

symporter (Supplementary Table 4). These findings substantiate that marine bacteria can use multiple regulatory functions to maintain a favourable internal pH in the face of external stress induced by increased p_{CO_2}.

In bacteria, a variety of molecular mechanisms to cope with acid stress have been identified[20,21]. Altogether, pH homeostasis-related genes represented 26 of the 113 genes with significantly higher relative abundances in the acidified Low-Chl mesocosms compared with controls (representing 20.7% of the differentially expressed transcripts), although pH also slowly decreased over time in the controls, albeit less than in the acidified mesocosms (Fig. 1a). In contrast, out of 190 genes with significantly lower relative abundances under acidification, only 8 genes were pH homeostasis-related (representing 0.2% of transcripts; Supplementary Fig. 3). Among the non-homeostasis-related genes negatively affected by acidification, we note an array of phage genes, dominated by transcripts most similar to Podoviridae family phages infecting SAR11-clade bacteria. In the High-Chl mesocosms, none of the significantly higher expressed genes in response to elevated CO_2 had known functions in pH homeostasis (Supplementary Table 3). The very low differential expression of pH homeostasis genes in the High-Chl mesocosms most likely resulted from the general increase in pH, driven by high photosynthetic activity. Pronounced increases in pH are typical for natural phytoplankton blooms[25]. Our findings indicate that pH in the acidified High-Chl mesocosms potentially increased above a critical threshold value where pH homeostasis responses were not required for regular bacterial cell functioning. Alternatively, pH homeostasis gene expression responses in the High-Chl mesocosms could have been masked by high expression of genes responding to the decaying phytoplankton bloom[25,26]. Nevertheless, under either scenario, our findings show that bacteria invest a substantially larger proportion of their transcriptional effort to pH homeostasis mechanisms under Low-Chl compared with High-Chl conditions. This implies that increased expression of pH homeostasis genes could represent a critical strategy for bacterial adjustment to lowered pH in low-chlorophyll, oligotrophic marine environments.

To uncover ecological effects of elevated CO_2 on particular components of bacterioplankton communities, we analysed the gene expression responses of the four most abundant bacterial groups in the mesocosms (Fig. 1e). These groups represent bacteria with highly different physiologies and ecological life strategies. Thus, whereas the Alteromonadaceae (Gammaproteobacteria), Flavobacteriaceae (Bacteroidetes), and the Roseobacter clade (Alphaproteobacteria) are typically associated with organic matter degradation during or following both natural and experimentally induced phytoplankton blooms[27,28], the SAR11 clade (Alphaproteobacteria) represents oligotrophic bacteria that are persistently abundant in the world's oceans. In the Low-Chl mesocosms, 8.2–17.0% of the transcripts assigned to each of the Alteromonadaceae, SAR11 and Flavobacteriaceae were significantly differentially expressed in response to acidification. Their corresponding proportion in the High-Chl mesocosms was <4.2%. Roseobacters showed lower proportions in both the Low- and High-Chl mesocosms (averaging 5.3% and 1.6%, respectively). Notably, for all investigated taxa, genes involved in pH homeostasis regulation accounted for 5.1–35.3% of the transcripts of genes with significantly higher relative abundance in acidified compared with control Low-Chl mesocosms. In contrast, no such differential responses to elevated CO_2 were observed for pH homeostasis genes in the High-Chl mesocosms.

Interestingly, the differentially expressed genes involved in pH homeostasis varied among bacterial taxa (Fig. 3 and Supplementary Fig. 4 and Supplementary Tables 2 and 3). Thus, for Alteromonadaceae, acidification-induced transcription under Low-Chl conditions primarily involved genes encoding four out of five electron transport complexes. For roseobacters, the most responsive genes encoding proton pumping proteins were ATP synthase C chain, cytochrome *c*-type biogenesis protein CcmC, and the gamma subunit of formate dehydrogenase. For the SAR11 clade and Flavobacteriaceae, pyrophosphate-energized proton pump and ATP synthase C chain, respectively, were the most abundant among differentially expressed genes with potential roles in pH homeostasis. Given that bacteria in extended ocean regions are energy limited[29], it is pertinent to resolve how differences in bioenergetic requirements of different pH homeostasis mechanisms affect the metabolism of dominant bacterioplankton groups.

Until present, most studies assessing acidification effects on bacterioplankton were done in experimental contexts of nutrient-induced phytoplankton blooms (but see ref. 8 for experiments without nutrient enrichment). However, the authors of ref. 25 recently suggested that consequences of ocean acidification on marine biota may be most pronounced in the oligotrophic open ocean compared

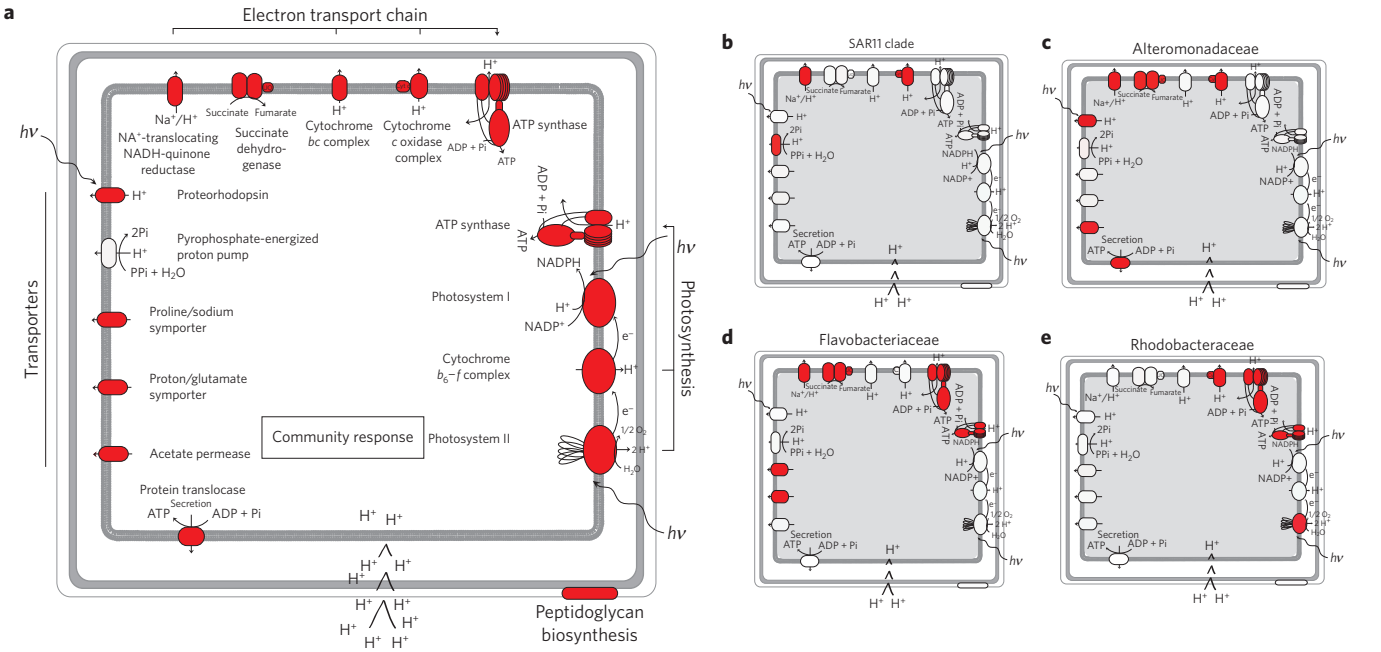

Figure 3 | Model of bacterial strategies for pH homeostasis on acid stress. a, Model of the whole bacterial community. **b**–**e**, Genes of the SAR11 clade (**b**), Alteromonadaceae (**c**), Flavobacteriaceae (**d**) and Rhodobacteraceae (**e**). The proteins remain in the same position in all panels. All proteins involved in maintaining pH homeostasis that showed significantly higher relative expression of at least one gene in Low-Chl-acidified mesocosms (pH 7.8) are shown in red. References for identification of pH homeostasis-related genes are in Supplementary Table 4.

with more nutrient-rich coastal waters and upwelling areas where high-chlorophyll phytoplankton blooms naturally cause substantial increases in pH. Accordingly, we observed more pronounced gene expression responses to elevated CO_2 in the Low-Chl compared with High-Chl mesocosms. Moreover, our findings suggest a series of molecular mechanisms by which marine bacteria attempt to meet the physiological challenge imposed by pH stress. Given that bacterial abundance and production was maintained despite the change in pH, our transcriptional analyses would indicate that physiological acclimation of bacteria to elevated CO_2 is possible. However, the observed mechanisms to export protons across the cell membrane are inherently energy demanding. In the context of ocean acidification, this implies that bacteria would need to allocate more energy to cell maintenance instead of growth. Resulting changes in bacterial growth efficiency could thus influence bacterial carbon cycling and energy fluxes in the microbial food web. In fact, mesocosm studies extended over several weeks report significant effects of elevated CO_2 on bacterial activity measures determining biogeochemical process rates[8–10,12,13]. We posit that understanding pH homeostasis mechanisms is essential for interpreting how marine bacteria and their biogeochemical cycling services will respond to projected levels of ocean acidification at relevant scales[30] and over extended time periods in oceanic environments.

Methods

Methods and any associated references are available in the online version of the paper.

Received 25 June 2015; accepted 27 November 2015; published online 11 January 2016

References

1. Azam, F. Microbial control of oceanic carbon flux: the plot thickens. *Science* **280,** 694–696 (1998).
2. Hennon, G. M. M. *et al.* Diatom acclimation to elevated CO_2 via cAMP signalling and coordinated gene expression. *Nature Clim. Change* **5,** 761–765 (2015).
3. Lohbeck, K. T., Riebesell, U. & Reusch, T. B. Adaptive evolution of a key phytoplankton species to ocean acidification. *Nature Geosci.* **5,** 346–351 (2012).
4. Tagliabue, A., Bopp, L. & Gehlen, M. The response of marine carbon and nutrient cycles to ocean acidification: large uncertainties related to phytoplankton physiological assumptions. *Glob. Biogeochem. Cycles* **25,** GB3017 (2011).
5. Pelejero, C., Calvo, E. & Hoegh-Guldberg, O. Paleo-perspectives on ocean acidification. *Trends Ecol. Evol.* **25,** 332–344 (2010).
6. Bopp, L. *et al.* Multiple stressors of ocean ecosystems in the 21st century: projections with CMIP5 models. *Biogeosciences* **10,** 6225–6245 (2013).
7. Häder, D. P. & Gao, K. Interactions of anthropogenic stress factors on marine phytoplankton. *Front. Environ. Sci.* **3,** 14 (2015).
8. Krause, E. *et al.* Small changes in pH have direct effects on marine bacterial community composition: a microcosm approach. *PLoS ONE* **7,** e47035 (2012).
9. Grossart, H. P., Allgaier, M., Passow, U. & Riebesell, U. Testing the effect of CO_2 concentration on the dynamics of marine heterotrophic bacterioplankton. *Limnol. Oceanogr.* **51,** 1–11 (2006).
10. Arnosti, C. *et al.* Dynamics of extracellular enzyme activities in seawater under changed atmospheric p_{CO_2}: a mesocosm investigation. *Aquat. Microb. Ecol.* **64,** 285–298 (2011).
11. Allgaier, M. *et al.* Coupling of heterotrophic bacteria to phytoplankton bloom development at different p_{CO_2} levels: a mesocosm study. *Biogeosciences* **5,** 1007–1022 (2008).
12. Lindh, M. V. *et al.* Consequences of increased temperature and acidification on bacterioplankton community composition during a mesocosm spring bloom in the Baltic Sea. *Environ. Microbiol. Rep.* **5,** 252–262 (2013).
13. Piontek, J. *et al.* Acidification increases microbial polysaccharide degradation in the ocean. *Biogeosciences* **7,** 1615–1624 (2010).
14. Robinson, C. & Williams, P. J. B. in *Respiration in Aquatic Ecosystems* (eds del Giorgio, P. A. & Williams, P. J. B.) 147–181 (Oxford Univ. Press, 2005).
15. Field, C. B. *et al.* (eds) *Impacts, Adaptation, and Vulnerability. Part A: Global and Sectoral Aspects* (IPCC, Cambridge Univ. Press, 2014).
16. Sala, M. M. *et al.* Contrasting effects of ocean acidification on the microbial food web under different trophic conditions. *ICES J. Mar. Sci.* http://dx.doi.org/10.1093/icesjms/fsv130 (2015).
17. Baltar, F. *et al.* Response of rare, common and abundant bacterioplankton to anthropogenic pertubations in a Mediterranean coastal site. *FEMS Microbiol. Ecol.* **91,** fiv058 (2015).
18. Shibata, C. *et al.* Gene structure of *Enterococcus hirae* (*Streptococcus faecalis*) F1FO-ATPase, which functions as a regulator of cytoplasmic pH. *J. Bacteriol.* **174,** 6117–6124 (1992).

19. Spero, M. A., Aylward, F. O., Currie, C. R. & Donohue, T. J. Phylogenomic analysis and predicted physiological role of the proton-translocating NADH: quinone oxidoreductase (complex I) across bacteria. *mBio* **6,** e00389–e00415 (2015).
20. Maurer, L. M. *et al.* pH regulates genes for flagellar motility, catabolism, and oxidative stress in *Escherichia coli* K-12. *J. Bacteriol.* **187,** 304–319 (2005).
21. Mangold, S., Jonna Rao, V. & Dopson, M. Response of *Acidithiobacillus caldus* toward suboptimal pH conditions. *Extremophiles* **17,** 689–696 (2013).
22. Gómez-Consarnau, L. *et al.* Light stimulates growth of proteorhodopsin-containing marine Flavobacteria. *Nature* **445,** 210–213 (2007).
23. Akram, N. *et al.* Regulation of proteorhodopsin gene expression by nutrient limitation in the marine bacterium *Vibrio* sp. AND4. *Environ. Microbiol.* **15,** 1400–1415 (2013).
24. Fuhrman, J. A., Schwalbach, M. S. & Stingl, U. Proteorhodopsins: an array of physiological roles? *Nature Rev. Microbiol.* **6,** 488–494 (2008).
25. Duarte, C. M. *et al.* Is ocean acidification an open-ocean syndrome? Understanding anthropogenic impacts on seawater pH. *Estuar. Coast.* **36,** 221–236 (2013).
26. Spilling, K. Dense sub-ice bloom of dinoflagellates in the Baltic Sea, potentially limited by high pH. *J. Plankton Res.* **29,** 895–901 (2007).
27. Buchan, A., LeCleir, G., Gulvik, C. & González, J. Master recyclers: features and functions of bacteria associated with phytoplankton blooms. *Nature Rev. Microbiol.* **12,** 686–698 (2014).
28. Teeling, H. *et al.* Substrate-controlled succession of marine bacterioplankton populations induced by a phytoplankton bloom. *Science* **336,** 608–611 (2012).
29. Del Giorgio, P. A. *et al.* Coherent patterns in bacterial growth, growth efficiency, and leucine metabolism along a northeastern Pacific inshore-offshore transect. *Limnol. Oceanogr.* **56,** 1–16 (2011).
30. Riebesell, U. & Gattuso, J. P. Lessons learned from ocean acidification research. *Nature Clim. Change* **5,** 12–14 (2015).

Acknowledgements

The skilful technical assistance of S. Arnautovic, V. Balague, C. Cardelús, L. Cros, E. Vázquez-Domínguez, J. Movilla and À. López-Sanz made this experiment possible. We thank Anselm and the CEAB boat crew for assistance with sampling and M. A. Moran for insightful comments on our work. This research was financially supported by grants from the Göran Gustafsson Foundation for Research in Natural Sciences and Medicine, the Swedish Research Council VR, the Swedish Research Council FORMAS strong research programme EcoChange, and the BONUS BLUEPRINT project, which has received funding from BONUS, the joint Baltic Sea research and development programme (Art 185), funded jointly from the European Union's Seventh Programme for research, technological development and demonstration and from the Swedish Research Council FORMAS to J.Pinhassi. The research was also financially supported by the Spanish Ministry of Science and Innovation project DOREMI (CTM2012-34294) to C.M. and J.M.Gasol, and by project CTM2013-48292-C3-3-R to J.M.Gasol.

Author contributions

M.D., C.P., J.M.Gasol and J.Pinhassi conceived the study. C.P., C.M., J.M.Gasol and J.Pinhassi designed research. N.A., M.V.-C., J.M.González, E.C., C.P., C.M., J.M.Gasol and J.Pinhassi carried out the mesocosm experiment and collected samples for microbial and chemical analyses. E.C. and C.M. measured and adjusted pH. N.A., M.V.-C. and J.Palovaara carried out RNA extraction. C.B., D.L., C.M.G.K., L.S., K.H., J.M.González, M.D. and J.Pinhassi analysed data. C.B., D.L. and J.Pinhassi wrote the paper with help from C.M.G.K., L.S. and M.D. All authors discussed the results and commented on the manuscript.

Additional information

Supplementary information is available in the online version of the paper. Reprints and permissions information is available online at www.nature.com/reprints. Correspondence and requests for materials should be addressed to J.Pinhassi.

Competing financial interests

The authors declare no competing financial interests.

Methods

Experimental set-up. Two thousand litres of surface water (1 m depth) was collected from 1 km off the coast of Catalonia at the Blanes Bay Microbial Observatory (41° 40′ N, 2° 48′ E; Spain) on 2 February 2010. The *in situ* chlorophyll *a* concentration was 0.75 μg l^{-1} and the temperature was 14 °C. The sea water was filtered through a 200 μm mesh to remove large zooplankton, enclosed in two containers and transported to a climate chamber where the water was divided into eight, 200 l polyethylene mesocosms. Four mesocosms were maintained without nutrient enrichment, to maintain low phytoplankton biomass (where biomass is typically inferred from chlorophyll *a* concentrations) representative of the northwestern Mediterranean at the time of the experiment—these mesocosms are hereafter referred to as Low-Chl mesocosms. Out of the Low-Chl mesocosms, duplicate mesocosms were acidified by bubbling with CO_2 (Low-Chl-acidified) and duplicate mesocosms were left untreated serving as controls (Low-Chl-control). To investigate bacterioplankton responses to elevated CO_2 in waters with contrasting trophic status, the remaining four mesocosms were enriched with nutrients to induce phytoplankton blooms (reaching chlorophyll *a* concentrations typical of coastal upwelling systems). These mesocosms are hereafter referred to as the High-Chl mesocosms. The nutrient-enriched mesocosms received final concentrations of 1 μM P as Na_2HPO_4, 16 μM N as $NaNO_3$, and 30 μM Si as $NaSiO_3$. For N, this corresponds to eight times the annual average concentration in Blanes Bay during February; P was added in Redfield ratio to N; and Si was added in excess to assure no Si limitation of diatoms. Out of the four High-Chl mesocosms, duplicate mesocosms were acidified (High-Chl-acidified) and duplicate mesocosms served as nutrient-enriched controls without acidification (High-Chl-control).

The pH in the mesocosms was determined by spectrophotometry in the laboratory, after the addition of *m*-cresol purple according to the methodology in ref. 31. Samples for pH measurements were collected every morning at around 10:00, at the time of sampling for chemical and biological variables. Based on the spectrophotometry pH measurements, adjustment of pH in the acidified mesocosms was performed by bubbling with minute volumes of CO_2 (99.9% purity) after sampling for chemical and biological variables, and was manually regulated to maintain the pH in the acidified tanks approximately 0.20 pH units lower than in the controls. Control mesocosms without acidification were bubbled with equal volumes of compressed air at contemporary atmospheric CO_2 concentration. In addition to the spectrophotometric pH measurements, pH in the acidified mesocosms was continuously measured using glass electrodes (LL Ecotrode plus-Metrohm), which were Tris buffer-calibrated daily, following standard procedures of ref. 32, and data were recorded by a D130 data logger (Consort; Supplementary Fig. 5). pH measurements by spectrophotometry are more precise than data obtained using glass electrodes. Still, continuous pH monitoring using the electrodes allowed the assessment of natural and experimentally induced pH fluctuations during the experiment (see legend to Supplementary Fig. 5 for detail).

The mesocosms were incubated for 9 days at 14 °C on a 12:12 h light/dark cycle. Light intensity inside the mesocosms was 121.3 ± 3.5 μmol m^{-2} s^{-1}, provided by a combination of cool-white and Gro-Lux fluorescent lamps.

Bacterial abundance and heterotrophic production. Samples for bacterial abundance and heterotrophic production were collected in the morning on a daily basis. Bacterial abundance was determined by flow cytometry. The samples were fixed with 1% paraformaldehyde and 0.05% glutaraldehyde and stored at −70 °C. Samples were stained using 10× SybrGreen I before being counted in a FACSCalibur flow cytometer (BD Biosciences). Heterotrophic bacterial production was estimated using [^{3}H]leucine incorporation[33,34]. For each sample, triplicate aliquots (1.2 ml) and a trichloroacetic acid-killed control were incubated with 40 nM [^{3}H]leucine for 1 h at 14 °C in the dark. A theoretical conversion factor of 1.55 kg C mol leucine^{-1} was used to convert leucine incorporation rates to bacterial carbon production.

Chlorophyll *a* concentration. For the quantification of chlorophyll, as a proxy for algal biomass, 50 ml of sample was collected in the morning on a daily basis, immediately filtered through Whatman GF/F glass fibre filters, and subsequently extracted in acetone (90%). The samples were incubated in the dark (for 24 h at 4 °C). Concentrations were measured using a Turner Designs fluorometer[35].

RNA sample collection and processing. Water samples for microbial mRNA community-wide gene expression analysis were collected from the mesocosms in the morning of Day 9. The day for RNA sample collection was chosen on the basis of insights into bacterioplankton responses in previous mesocosm experiments in the northwestern Mediterranean Sea[36,37]. These studies show that bacterial responses in activity and abundance are pronounced ∼2 days after nutrient-induced peaks in chlorophyll *a* concentration; thus allowing comparisons between responses of bacterioplankton communities under different trophic conditions. Between 11–20 l of water from each mesocosm (lowest volumes from the nutrient-enriched mesocosms, owing to the higher microbial biomass resulting in clogging of filters) was pre-filtered through a 5-μm-pore-size 142-mm-diameter polycarbonate filter and the cells were collected on a 0.2-μm-pore-size 142-mm-diameter filter. Total filtration time was <25 min per sample. Filters were put in 15 ml Falcon tubes containing 2 ml Buffer RLT (containing 10 μl beta-mercaptoethanol per millilitre) and flash frozen in liquid nitrogen before storage at −80 °C. mRNA was extracted essentially according to the protocol of ref. 38, using the RNEasy kit (Qiagen). Genomic DNA was removed using the TURBO DNA-free kit (Ambion) and ribosomal RNA was removed enzymatically using mRNA-ONLY prokaryotic mRNA isolation kit (Epicenter Biotechnologies) and MICROBExpress (Ambion) according to the manufacturers' recommendations. Bacterial mRNA was further enriched using MICROBEnrich (Ambion). cDNA synthesis from mRNA was carried out using AMBION message Amplification II-Bacteria kit (Ambion). The MessageAmp II-Bacteria Kit (Ambion) was used to linearly amplify RNA. cDNAs from each sample were sequenced using the HiSeq 2000 sequencing system (Illumina) at SciLifeLab Stockholm.

Bioinformatics. The generated Illumina sequences were quality checked, trimmed, and filtered against the Silva database of small and large subunit ribosomal RNA (ref. 39) using the filtering mode of the Erne mapper[40] with default parameters. Subsequently, all samples were individually assembled using the Ray[41] and Velvet[42] assemblers with kmer length settings varying between 21 and 95 for the former and 31 and 87 for the latter. Open reading frames (ORFs) were called on resulting contigs using FragGeneScan[43] with settings for Sanger sequences as sequences were assembled. The resulting ORFs were clustered before annotation to remove duplicates using Usearch[44]. Subsequently, the resulting ORFs were annotated using BLAST[45] against the M5NR SEED, KEGG, and RefSeq databases[46], followed by annotation using in-house developed scripts (available at https://github.com/erikrikarddaniel/environmentmicrobedb-tools). ORF sequences with BLAST hits with bitscores ≥35 were functionally annotated and taxonomic annotation was carried out using the LCA algorithm[47], considering all hits within 0.9 times the bitscore of the best hit. Annotated ORFs are referred to as 'genes' in the biological context of expression. Some genes in public databases may actually represent ribosomal RNA rather than protein coding genes, and are potentially missed in standard sequence filtration procedures[48]. In our data set, we identified three genes representing 23S rRNA genes that had been incorrectly annotated as functional genes in SEED. These were 'cell-wall associated hydrolase', 'retron-type reverse transcriptase' and 'Zn-dependent protease with chaperone function', which were then removed from further analyses. As seen in Supplementary Table 1, our annotation pipeline resulted in between 19–51% annotated sequences, which is similar to other studies on complex marine microbial communities showing annotation percentages between, for example, 8–71%, with values often around 20–30% (refs 49–52).

To quantify annotated ORFs/genes, the original sequences were mapped back against annotated ORFs using Bowtie 2 (ref. 53) in end-to-end mode. Sequence read counts were summed over ORFs/genes with identical annotation for the community, resulting in quantitative assessment of individual expressed genes in each sample. For comparison of gene expression levels between samples, relative transcript abundances for each gene were calculated by dividing the number of transcript reads per gene by the number of annotated reads per sample. These relative transcript abundances are presented as counts per million (CPM). For the four major taxa in the mesocosms (Alteromonadaceae, Flavobacteriaceae, Rhodobacteraceae and SAR11; that is, taxa delimited roughly at the family level that accounted for >0.5% of the annotated reads in each of the treatments), we calculated taxon-specific relative transcript abundances for each gene by dividing the number of transcript reads per gene for each taxon by the number of total annotated reads for the respective taxon per sample (these results are also presented as CPM). It should be noted that functional annotation and assessment of gene expression patterns in metatranscriptomics are challenging at the species level owing to a general lack of reference genomes for marine bacteria. Further, it is unknown how genomic microdiversity within a species (for example, copy number variability of protein encoding genes between closely related genotypes defined by 16S rRNA gene sequences) would affect interpretations of gene expression patterns in natural microbial communities.

Statistical analysis of differentially expressed transcripts was performed using the R package EdgeR (ref. 54) after removal of ORFs identified only as 'putative proteins'. The EdgeR analysis was based on sequence read counts, to which default normalization factors as well as common and tagwise dispersal factors were applied before the exact test was performed. As a result of the exact test, for each gene EdgeR determines a logarithm base 2 estimate of counts per million (logCPM) and a logarithm base 2 estimate of fold change in relation to the logCPM value. The EdgeR analysis includes a *p* value calculation and a false discovery rate for each gene in a data set, but does not exclude false positives. We extracted differentially expressed genes at a significance level of $p < 0.01$. As an additional quality control step of genes detected as significantly differently expressed in EdgeR, we required that the calculated relative transcript abundance (CPM) in both replicates of the acidified mesocosms had to be 1.5 times higher compared with the average of the

non-acidified controls; or alternatively, that both replicates of the non-acidified mesocosms had to be 1.5 times higher compared with the average of the acidified controls.

ORFs of differentially expressed genes potentially deriving from phages were searched with Usearch v. 8 (ref. 44) against NCBI's collection of viral genomes (February 2015). Three genes annotated as ORFs with nucleotide sequence similarity to a phiX genome were discovered: 'Phage protein', 'Phage major capsid protein', and 'DNA maturase, phage-associated'. Being a potential contamination from added phiX DNA during sequencing, the phiX sequences were removed from the list of differentially expressed genes. For taxonomic identification of other phage transcripts, original sequences of the ORFs annotated as phages in SEED, which were also significantly differentially expressed in response to acidification, were annotated in MEGAN. This showed that among a total of 1,692 phage ORFs, 1,093 ORFs could be taxonomically identified at the family level. These were 108 Myoviridae ORFs, 137 Siphoviridae ORFs, and 848 Podoviridae ORFs. Genes with known roles in pH homeostasis were identified by manually going through literature for the significantly differentially expressed genes (for references, see Supplementary Table 4).

The sequence data generated in the present study were deposited in the European Nucleotide Archive (http://www.ebi.ac.uk/ena/data/view/PRJEB10237) under project number PRJEB10237.

Gene names and abbreviations in Fig. 2. Gene names and abbreviations for SEED4-level annotations: *actP*, acetate permease ActP (cation/acetate symporter); *araC*, transcriptional regulator AraC family; *atpC*, ATP synthase C chain; ccmC, cytochrome *c*-type biogenesis protein CcmC; *ccoN*, cytochrome *c* oxidase subunit CcoN; *coxN*, alternative cytochrome *c* oxidase polypeptide coxN; ctp, putative TEGT family carrier/transport protein; dbp, DNA-binding protein; dctm, TRAP dicarboxylate transporter, DctM subunit; dds, dehydrogenases with different specificities; ehvd, enoyl-CoA hydratase [valine degradation]; fig3573, FIG003573: hypothetical protein; fld, flavodoxin; *fleQ*, flagellar regulatory protein fleQ; *gltK*, glutamate aspartate transport system permease protein gltK; glyX, glycoprotein X precursor; hcbr, haemolysin-type calcium-binding region; hyp, hydantoin permease; ioppp, inorganic pyrophosphatase; *l3p*, protein-N(5)-glutamine methyltransferase prmB, methylates LSU ribosomal protein L3p; *lonP*, uncharacterized protein, similar to the amino-terminal domain of Lon protease; *moaA*, molybdenum cofactor biosynthesis protein moa; mor, molybdopterin oxidoreductase; *mraY*, phospho-*N*-acetylmuramoyl-pentapeptide-transferase; mtsp, ABC-type multidrug transport system, permease component; *mxaF*, methanol dehydrogenase large subunit protein; *nqrB*, Na^+-translocating NADH-quinone reductase subunit B; *nqrE*, Na^+-translocating NADH-quinone reductase subunit E; nuct, nucleoside transporter; nuSN, nuclease (SNase-like); oacps, 3-oxoacyl[acyl-carrier-protein] synthase KAS II; *oprO*, pyrophosphate-specific outer membrane porin OprO; pa3071, PA3071 hypothetical protein; pcf, Zn-dependent protease with chaperone function; *pet*, cytochrome b_6–f complex subunit, cytochrome b_6; pfp, xanthine/uracil/thiamine/ascorbate permease family protein; phap, phasin PhaP; *prd*, proteorhodopsin; *psaC*, photosystem I iron–sulphur centre subunit VII (psaC); *psbC*, photosystem II 44 kDa subunit reaction centre protein; *rbc*, ribulose bisphosphate carboxylase; rtx, RTX toxins and related Ca^{2+}-binding proteins; sdgt, predicted sodium-dependent galactose transporter; *sdhD*, succinate dehydrogenase hydrophobic membrane anchor protein; *secD*, protein-export membrane protein secD; secE, preprotein translocase subunit secE; soh, shut off host DNA synthesis protein; str, sulphate transporter; strp, type I secretion target repeat protein; ttdt, TRAP-type C4-dicarboxylate transport system, small permease component.

References

31. Clayton, T. D. & Byrne, R. H. Spectrophotometric seawater pH measurements: total hydrogen ion concentration scale calibration of m-cresol purple and at-sea results. *Deep-Sea Res. I* **40,** 2115–2129 (1993).
32. Dickson, A. G., Sabine, C. L. & Christian, J. R. *Guide to Best Practices for Ocean CO_2 Measurements* Vol. 3 (PICES Special Publication, 2007).
33. Kirchman, D., K'nees, E. & Hodson, R. Leucine incorporation and its potential as a measure of protein synthesis by bacteria in natural aquatic systems. *Appl. Environ. Microbiol.* **49,** 599–607 (1985).
34. Smith, D. C. & Azam, F. A simple, economical method for measuring bacterial protein synthesis rates in seawater using 3H-leucine. *Mar. Microb. Food Webs* **6,** 107–114 (1992).
35. Yentsch, C. S. & Menzel, D. W. A method for the determination of phytoplankton chlorophyll and phaeophytin by fluorescence. *Deep-Sea Res. I* **10,** 221–231 (1963).
36. Allers, E. *et al.* Response of *Alteromonadaceae* and *Rhodobacteriaceae* to glucose and phosphorus manipulation in marine mesocosms. *Environ. Microbiol.* **9,** 2417–2429 (2007).
37. Pinhassi, J. *et al.* Changes in bacterioplankton composition under different phytoplankton regimes. *Appl. Environ. Microbiol.* **70,** 6753–6766 (2004).
38. Poretsky, R. S. *et al.* Comparative day/night metatranscriptomic analysis of microbial communities in the North Pacific subtropical gyre. *Environ. Microbiol.* **11,** 1358–1375 (2009).
39. Quast, C. *et al.* The SILVA ribosomal RNA gene database project: improved data processing and web-based tools. *Nucleic Acids Res.* **41,** D590–D596 (2012).
40. Del Fabbro, C., Scalabrin, S., Morgante, M. & Giorgi, F. M. An extensive evaluation of read trimming effects on illumina NGS data analysis. *PLoS ONE* **8,** e85024 (2013).
41. Boisvert, S. *et al.* Ray Meta: scalable *de novo* metagenome assembly and profiling. *Genome Biol.* **13,** R122 (2012).
42. Zerbino, D. R. & Birney, E. Velvet: algorithms for *de novo* short read assembly using de Bruijn graphs. *Genome Res.* **18,** 821–829 (2008).
43. Rho, M., Tang, H. & Ye, Y. FragGeneScan: predicting genes in short and error-prone reads. *Nucleic Acids Res.* **38,** e191 (2010).
44. Edgar, R. C. Search and clustering orders of magnitude faster than BLAST. *Bioinformatics* **26,** 2460–2461 (2010).
45. Altschul, S. F. *et al.* Gapped BLAST and PSI-BLAST: a new generation of protein database search programs. *Nucleic Acids Res.* **25,** 3389–3402 (1997).
46. Overbeek, R. *et al.* The subsystems approach to genome annotation and its use in the project to annotate 1000 genomes. *Nucleic Acids Res.* **33,** 5691–5702 (2005).
47. Huson, D. H., Auch, A. F., Qi, J. & Schuster, S. C. MEGAN analysis of metagenomic data. *Genome Res.* **17,** 377–386 (2007).
48. Tripp, J. H. *et al.* Misannotations of rRNA can now generate 90% false positive protein matches in metatranscriptomic studies. *Nucleic Acids Res.* **39,** 8792–8802 (2011).
49. Rivers, A. R. *et al.* Transcriptional response of bathypelagic marine bacterioplankton to the Deepwater Horizon oil spill. *ISME J.* **7,** 2315–2329 (2013).
50. Satinsky, B. M. *et al.* The Amazon continuum dataset: quantitative metagenomic and metatranscriptomic inventories of the Amazon River plume, June 2010. *Microbiome* **2,** 17 (2014).
51. Beier, S., Rivers, A. R., Moran, M. A. & Obernosterer, I. Phenotypic plasticity in heterotrophic marine microbial communities in continuous cultures. *ISME J.* **9,** 1141–1151 (2015).
52. Marchetti, A. *et al.* Comparative metatranscriptomics identifies molecular bases for the physiological responses of phytoplankton to varying iron availability. *Proc. Natl Acad. Sci. USA* **109,** E317–E325 (2011).
53. Langmead, B. & Salzberg, S. L. Fast gapped-read alignment with Bowtie 2. *Nature Methods* **9,** 357–359 (2012).
54. Robinson, M. D., McCarthy, D. J. & Smyth, G. K. edgeR: a Bioconductor package for differential expression analysis of digital gene expression data. *Bioinformatics* **26,** 139–140 (2010).